Switchable nonlinear metasurfaces for absorbing high power surface waves

Sanghoon Kim,[1,a)] Hiroki Wakatsuchi,[2] Jeremiah J. Rushton,[1] and Daniel F. Sievenpiper[1,b)]
[1]*Electrical and Computer Engineering Department, University of California at San Diego, La Jolla, California 92093, USA*
[2]*Department of Electrical and Electronic Engineering, Nagoya Institute of Technology, Gokiso-cho, Showa, Nagoya, Aichi 466-8555, Japan*

(Received 16 September 2015; accepted 12 January 2016; published online 26 January 2016)

We demonstrate a concept of a nonlinear metamaterial that provides power dependent absorption of incident surface waves. The metasurface includes nonlinear circuits which transform it from a low loss to high loss state when illuminated with high power waves. The proposed surface allows low power signals to propagate but strongly absorbs high power signals. It can potentially be used on enclosures for electric devices to protest against damage. We experimentally verify that the nonlinear metasurface has two distinct states controlled by the incoming signal power. We also demonstrate that it inhibits the propagation of large signals and dramatically decreases the field that is leaked through an opening in a conductive enclosure. © *2016 AIP Publishing LLC*.
[http://dx.doi.org/10.1063/1.4940712]

Microwave technology has been developed extensively for wireless and satellite communications, as well as radar and other applications. With the increase in microwave applications, modern electronics and sensitive antennas are easily exposed to interference from external microwave signals. Specifically, when high power signals impinge on a conductive enclosure, surface currents can cause interference which triggers faults or malfunctions of the enclosed electronic devices.[1] The high power surface currents are capable of leaking inside through gaps or openings in the conductive shielding. Even if an aperture is electrically small, it can effectively behave as a slot antenna that can allow radiation inside.

Conventional approaches[2,3] to inhibit such destructive interference include applying a lossy coating on the outer surface of the metallic shielding. Another method is to use a resonant absorber such as a Salisbury screen,[4] Jaumann absorber,[5] or metamaterial absorber[6–9] to absorb incoming waves. Such conventional approaches based on linear materials absorb low power and high power signals equally. Thus, they can reduce the performance of antennas located on the surface and can affect the operation of a low power communication system. Moreover, surface currents are not entirely suppressed, and absorbing coatings can be characterized by their attenuation rate which depends on the thickness and the materials that make up the absorber.[10] One advantage of a nonlinear absorber is that it can decouple the attenuation of potentially damaging high power signals from the attenuation of low power signals that are needed for communication.

Here, we introduce the concept of a switchable metamaterial absorber based on nonlinear circuits integrated into a high impedance surface.[11] These surfaces are electrically thin, typically $\leq \lambda/10$, where λ is the free space wavelength.

Nonlinear metasurfaces which respond to the waveform and power of the incoming wave have previously been demonstrated.[12–14] Compared to prior works, this structure provides high power absorption regardless of the incoming waveform using a much simpler circuit, requiring only a single diode per cell, and no reactive components. Furthermore, we demonstrate nonlinear attenuation of surface waves over a large area and suppressed leakage of high power signals thorough a narrow gap by surrounding it with a nonlinear coating. We demonstrate this nonlinear absorber through electromagnetic/circuit co-simulation, validated by measurements of small samples inside waveguides, followed by large-area field measurements, and finally, a measurement of the reduction of electromagnetic fields entering an enclosure. Our measurements show surface wave attenuation that exceeds that of a conventional linear absorber, and the use of such a surface for practical applications.

The main mechanism of the switchable metasurface is that a metallic structure embedded with nonlinear devices such as diodes will change its conductive topology, and thus its absorbing properties, as a function of the incident power level. The structure shown in Fig. 1(a) is based on the high impedance surface,[11] which consists of conductive patches connected to a ground plane by vertical conducting vias. A pair of diodes is located at each vertical via, and a network of resistors is interconnected between the patches. Because of the nonlinear diodes, the metasurface transforms from one state to another depending on the power level, shown as the insets to Fig. 1(a). In order to facilitate fabrication, we used a planar geometry, in which the top patches of the metasurface are each composed of an outer ring and an inner patch connected with a via. Two diodes are connected in opposite polarity between the ring and the inner patch so that the surface will respond to both positive and negative portions of the RF cycle.

Surface waves generate currents in the patches, as well as voltages between the patches and the ground plane. At low power, the diodes appear as an open circuit.

[a)]Electronic mail: sak041@ucsd.edu
[b)]Electronic mail: dsievenpiper@eng.ucsd.edu

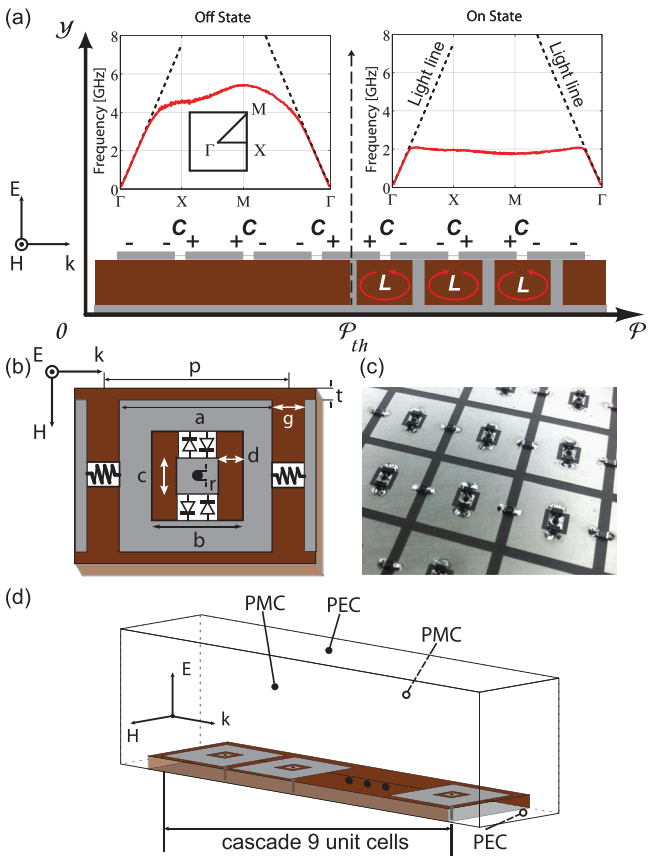

FIG. 1. Nonlinear metasurfaces for power dependent absorption: (a) Diagram of the metasurface with two distinct states defined by a threshold power. Insets of dispersion diagrams for the off- and on-states. (b) Geometry of the unit cell $p=17$, $t=3.175$, $g=2$, $a=15$, $b=4.49$, $c=2.762$, $d=0.864$, and $r=1.0$ (all in mm). (c) A photograph of the sample with circuit components attached. (d) A simulation model with a cascade of nine unit cells in a row with perfect magnetic conducting (PMC) walls to simulate a 2-D array.

However, when the voltage exceeds the turn-on voltage of the diodes, they behave as a short circuit, connecting the patches to the ground plane. In this state, the surface behaves as an artificial magnetic conductor, with an inductive current path (L) through the vias and a capacitance (C) defined by the gaps between the patches. The LC resonance of the structure creates high surface impedance,[11] and the dispersion curve bends over to become flat, shown as the inset of the *on-state* in Fig. 1(a). Near the LC resonance frequency of around 2 GHz, the surface waves are highly confined to the surface and interact strongly with the metallic structure. Near the band edge, the surface waves are also strongly absorbed by the resistors that are connected between the patches. In contrast, if the voltage on the patches does not exceed the turn-on voltage of the diodes, the surface appears as a simple capacitive sheet on a grounded dielectric substrate, and losses in the resistors are not significantly enhanced without the LC resonance.

The nonlinear metasurface is implemented as shown in Fig. 1(b). Periodic conductive patterns are printed on a Rogers 5870 substrate with a 3.175 mm thickness and with a 17 mm period as shown in Fig. 1(c). Eigenmode simulations of a single unit cell provide the band diagrams for the *off-* and *on-states* shown in the insets of Fig. 1(a). EM/circuit co-simulation of a periodic array of cells was used to determine the absorption properties. A pair of Schottky diodes packaged together (Avago HSMS-286C with parasitic of a series resistance 6 Ω, lead frame inductance 0.2 nH, coupling capacitance 0.035 pF, bondwire inductance 0.7 nH, package capacitance 0.03 pF, and lead frame capacitance 0.01) was attached at each via, and 220 Ω resistors were attached between the patches. In these simulations, a row of 9 unit cells was simulated inside a transverse electromagnetic (TEM) waveguide constructed with perfect electric conducting (PEC) and perfect magnetic conducting (PMC) boundaries on opposing walls of the guide as shown in Fig. 1(d). The TEM waveguide measured 17 mm wide to fit one unit cell, and 54.6 mm in height.

The measurement samples were fabricated with the same geometry as the simulation model, except with a sufficient number of lateral cells to fit within a standard rectangular metal TE waveguide. Two separate waveguide sizes (WR284 and WR430) were required to cover the frequency range from 1.7 to 4 GHz. The resulting sample sizes were 4×9 cells and 6×9 cells. Transmission and reflection were measured using power meters (Agilent N1911A) with high power signals provided by RF amplifiers (Ophir 5022 and 5193). Note that although a TEM waveguide was used in simulation, and a TE waveguide was used in the measurement, both have similar electric and magnetic field profiles and can be expected to identify similar performance trends.[12,13] The TEM waveguide allows a much simpler simulation, but the required boundary conditions are not available for experiments.

The simulation and measurement results are shown in Fig. 2. Absorption was calculated as $A(\omega) = 1 - T(\omega) - R(\omega)$ ($A(\omega)$: absorption, $T(\omega)$: transmission, and $R(\omega)$: reflection with frequency dependence (ω)). Note that reflection is negligible in all cases. Additionally, parasitic parameters of the circuit components (specifically in the diodes) contribute to a small frequency shift, so the parasitic values of the circuit components were also considered in the simulations. At the design frequency of 2.4 GHz, the lower power absorption is about 10%. With increasing power, the surface becomes resonant at 2.4 GHz, and the absorption increases to a maximum of 70% as shown in Fig. 2(a). The full width at half maximum (FWHM) absorptivity of the metasurface for on-state is 1.05 GHz from 1.95 to 3.1 GHz at the center frequency. The attenuation rate at 2.4 GHz is shown in Fig. 2(b) as a function of the incident power level. Below 100 mW, the surface is in the off-state. Above 10 W, the attenuation rate is saturated. To study the effect on surface waves in an open environment, we constructed a large area of the nonlinear metasurface, measuring 391 mm by 527 mm, and 23×31 unit cells. Fig. 3 shows the geometry of the measurement, as well as low and high power field plots for the nonlinear metasurface. We also measured the field profile on standard magnetic radar absorbing material, magRAM (SRC Tech. DD-11006) of the same thickness. We excited surface waves by launching them from an open-ended waveguide placed adjacent to one edge of the surface. The surface was placed in our near-field scanner, which consists of two linear position controllers arranged to provide x-y scanning over a 1 square meter area shown in Fig. 3(b). We scanned a small

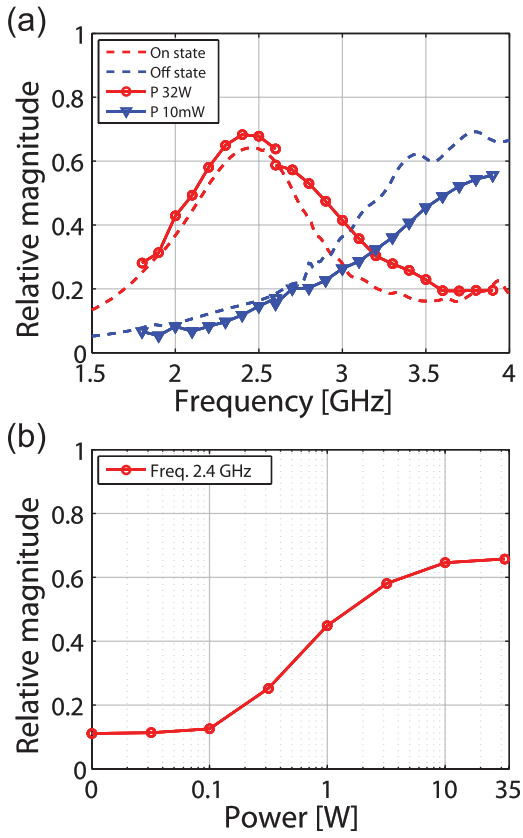

FIG. 2. Simulation and measurement of the nonlinear metasurface inside waveguide. The surface demonstrates two distinct states for low and high power conditions. (a) Dashed and solid dotted lines represent transient simulation and measurement data, respectively. (b) Absorption at 2.4 GHz versus incoming power levels.

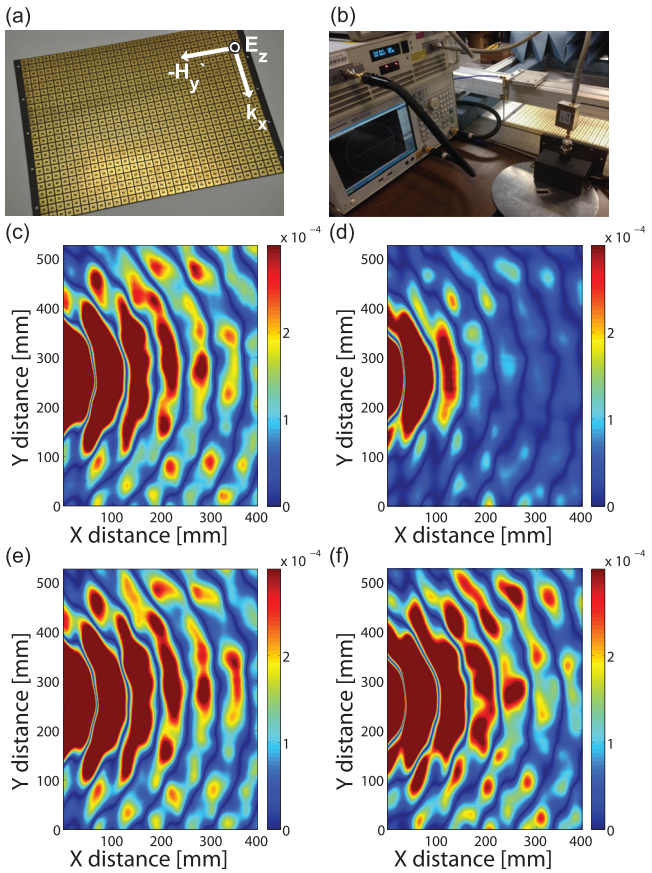

FIG. 3. Measurement of the surface field profiles under different power levels. (a) A large nonlinear metasurface, 391 × 527 (in mm). (b) The measurement setup with planar near field scanner, network analyzer (Agilent E5071C), and amplifier. A wave is launched near the center left edge of the surface. (c) Metasurface at 4.8 mW, (d) metasurface at 34 W, (e) magRAM at 4.8 mW, and (f) magRAM at 34 W.

coaxial probe over an area 2 mm above the surface to measure the electric field as a function of position for various power levels shown in Figs. 3(c)–3(f). The waveguide excites a surface wave that spreads out over the surface and is also attenuated by losses in the surface. As the power level is increased, the nonlinear metasurface shows increasing absorption, seen as reduced relative field strength from Figs. 3(c)–3(d). A transition to the highly absorbing state occurs at approximately 10 W of input power although the two plots represent two extremes of a continuous variation in absorption. The magRAM shows the same field profile for low and high field strength in Figs. 3(e) and 3(f), respectively. This is expected because it is a linear absorber. Unfortunately, it was not possible to extract the attenuation rate from these data because the reduction in field strength occurs due to both diffractions from the source and attenuation, with different regions of the surface having different attenuation rates.

In order to demonstrate the use of our nonlinear metasurface in a practical application, we constructed a metallic box with a narrow opening shown in Fig. 4(a). This would represent, for example, a piece of sensitive electronic equipment, a metallic shell of a vehicle, or some other conductive enclosure. Our assumption is that the enclosure may not be perfectly sealed, and external fields can leak in through small gaps, seams, or other openings. By covering the area around the gaps with a nonlinear absorber, one can limit the field level that is allowed to penetrate the box. For the following experiments, the box measured 560 × 910 × 100 (in mm) and a 9 mm wide opening was located on one face. We developed an experimental approach to measure the field leakage into the enclosure through the narrow opening and determine the effect of the nonlinear metasurface coating compared to a conventional magRAM coating as well as a bare metal surface. The metal box was placed in an anechoic chamber, and illuminated by 2.4 GHz waves from a horn antenna located on one wall of the chamber, 2.5 m away from the box as shown in Fig. 4(b). The signals from the network analyzer were amplified to as much as 150 W by a high power amplifier (Ophir 5265), and they impinged upon the box at a grazing angle relative to the face which contained the opening. The waves were vertically polarized relative to the top surface and propagated perpendicular to the gap in that surface. We used this geometry in order to efficiently excite transverse magnetic surface waves which could penetrate the gap.

We placed a small electric field probe inside the box below the opening and measured the field strength inside the box for various surface coatings. The field probe was calibrated by placing it at the same location without the box and using the Friis transmission equation. The field level inside the box is shown in Fig. 4(c) as a function of the impinging field strength for the nonlinear metasurface coating, compared to the conventional magRAM coating and to the bare

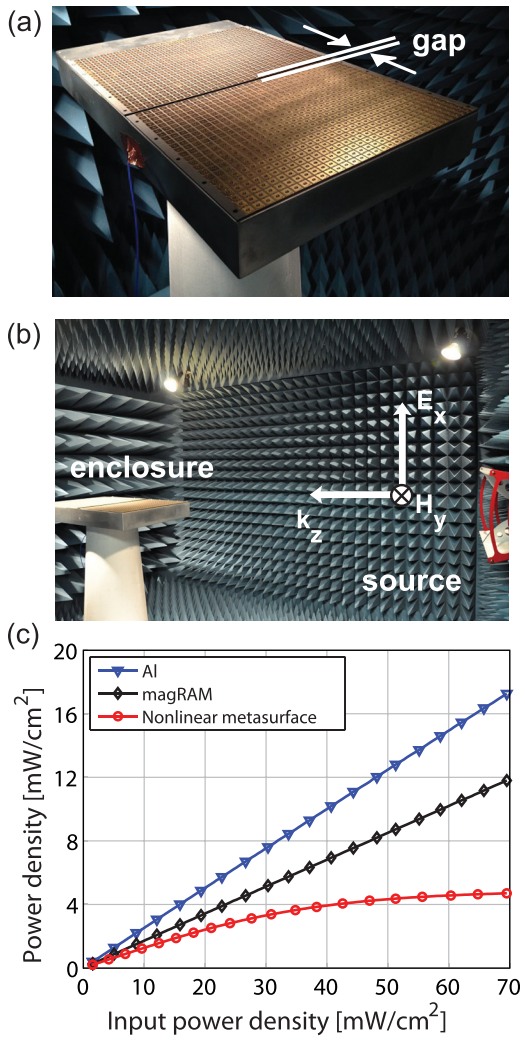

FIG. 4. (a) The metal enclosure with a gap in one face, surrounded by the nonlinear metasurface and compared to conventional magRAM and bare metal. (b) The measurement setup inside the anechoic chamber. (c) The field inside the enclosure as a function of the impinging field strength. The nonlinear metasurface demonstrates a saturation effect, limiting the field leakage into the enclosure.

metal surface. For both the metal surface and the magRAM, the field strength inside the box is a linear function of the external field strength, as expected because these are both linear materials. The magRAM shows a reduction in internal field strength relative to the bare metal case because of its absorption. However, the metasurface shows nonlinear absorption and exhibits a saturation effect, whereby the field inside the box is limited to roughly 4 mW/cm^2, regardless of the external field strength. Note also that the nonlinear metasurface coating provides substantially greater suppression of leakage than the magRAM coating, and its advantage increases with higher signal levels.

We also measured the signal strength for various gap sizes and for various probe positions inside the enclosure. In general, larger gaps allowed greater leakage for all three surfaces, as expected. Also, the field strength varied with position inside the box due to standing waves formed in the metal cavity, and it was generally reduced toward the back wall of the metal box. These variations may be reduced in future measurements by designing the box to be a single mode cavity at the frequency of interest. Nonetheless, the plot in Fig. 4(c) is representative of the trends seen in all cases, and we can conclude that the nonlinear metasurface coating provides not only an absorption advantage at its resonant frequency relative to a conventional magRAM but also a nonlinear saturation effect, limiting the field penetration through a gap in a metal enclosure.

In this letter, we have demonstrated a kind of nonlinear metasurface coating that changes its conductive topology in response to the power of the incoming wave. It converts from behaving as a simple capacitive sheet over a ground plane into a high impedance surface when the signal level surpasses the turn-on voltage of diodes at the vertical vias, and they become conductive. Resistors between the patches provide substantial absorption near the LC resonance frequency, which may be set by appropriate choice of the patch shape and substrate thickness. We have designed the surface to provide a significant absorption contrast at 2.4 GHz, and have demonstrated a change from 10% to 70% absorption with increasing power level, for small samples inside waveguides. Furthermore, we have performed planar near-field scans on electrically large surfaces. We have shown that at high power levels, the nonlinear metasurface can provide greater attenuation than a conventional magRAM coating near its design frequency. We have also shown that it can limit the amount of electromagnetic leakage through a gap in a metal enclosure, demonstrating that it can be used for practical applications.

This work was supported by the Office of Naval Research under Grant No. N00014-11-1-0460.

[1]D. F. Sievenpiper, IEEE Antennas Wireless Propag. Lett. **10**, 1516 (2011).
[2]G. T. Ruck, D. E. Barrick, W. D. Stuart, and C. K. Krichbaum, *Radar Cross Section Handbook* (Plenum Press, New York, New York, 1970).
[3]E. Knott, *Radar Cross Section Measurements* (SciTech Publishing, Raleigh, NC, 2006).
[4]W. W. Salisbury, "Absorbent body for electromagnetic waves," U.S. patent 2,599,944 (10 June 1952).
[5]B. A. Munk, *Frequency Selective Surfaces: Theory and Design* (Wiley–Interscience, New York, NY, 2000).
[6]N. I. Landy, S. Sajuyigbe, J. J. Mock, D. R. Smith, and W. J. Padilla, Phys. Rev. Lett. **100**, 207402 (2008).
[7]H. Tao, N. I. Landy, C. M. Bingham, X. Zhang, R. D. Averitt, and W. J. Padilla, Opt. Express **16**, 7181 (2008).
[8]H. Li, L. H. Yuan, B. Zhou, X. P. Shen, Q. Cheng, and T. J. Cui, J. Appl. Phys. **110**, 014909 (2011).
[9]F. Ding, Y. Cui, X. Ge, Y. Jin, and S. He, Appl. Phys. Lett. **100**, 103506 (2012).
[10]S. Kim and D. F. Sievenpiper, IEEE Trans. Antennas Propag. **62**, 475 (2014).
[11]D. F. Sievenpiper, L. Zhang, R. F. Broas, N. G. Alexopolous, and E. Yablonovitch, IEEE Trans. Microwave Theory Tech. **47**, 2059 (1999).
[12]H. Wakatsuchi, S. Kim, J. J. Rushton, and D. F. Sievenpiper, Appl. Phys. Lett. **102**, 214103 (2013).
[13]H. Wakatsuchi, S. Kim, J. J. Rushton, and D. F. Sievenpiper, Phys. Rev. Lett. **111**, 245501 (2013).
[14]Z. Luo, X. Chen, J. Long, R. Quarfoth, and D. F. Sievenpiper, IEEE Trans. Antennas Propag. **63**, 1736 (2015).